Resonant optical second-harmonic generation from mixed liquid crystal-stearic acid monolayers

1992 J. Phys.: Condens. Matter 4 7965

(http://iopscience.iop.org/0953-8984/4/40/008)

J. Phys.: Condens. Matter 4 (1992) 7965–7972. Printed in the UK

Resonant optical second-harmonic generation from mixed liquid crystal–stearic acid monolayers

Z-R Tang and J F McGilp†

Department of Pure and Applied Physics, Dublin University, Trinity College, Dublin, 2, Ireland

Received 19 May 1992

Abstract. Comparison of the linear and non-linear optical response of mixed liquid crystal/stearic acid molecular monolayers is used to show that significant geometric and electronic structural information can be extracted from the optical second-harmonic (SH) response. The combination of SH intensity and phase measurements provides much more information than intensity studies on their own, and adds an important spectroscopic dimension to SHG from molecular monolayers.

1. Introduction

Second-order non-linear optical techniques like second-harmonic generation (SHG) have recently been developed as extremely versatile and sensitive surface and interface probes [1–3]. A better understanding of the non-linear sources and the relation between the electronic structure and the non-linear optical response of surfaces, interfaces and thin films is required for the development and application of SHG in this area. Studies of simple model systems are particularly useful, and in this paper SHG from well characterized monolayers containing three structurally similar liquid crystals is used to investigate the relationship between the phase of the SH signal and nearby electronic resonances. Measurements of the phase of the SH signal from surfaces and thin films are rarely reported, although methods of measuring the SH phase by interferometry are known [4–6], and recently have been used under ultra-high-vacuum conditions for the first time [7]. As regards resonance effects, little has been done largely because of experimental difficulties associated with the tunable pulsed lasers required. Measurements on thin Rhodamine 110 films deposited from isopropanol solutions on glass substrates showed phase changes as the SH frequency approached an absorption peak of Rhodamine 110 as measured in isopropanol solution [8].

In this paper both the linear and non-linear optical response of well characterized monolayer films, deposited by the Langmuir–Blodgett technique, are measured directly, avoiding the potential problem of solvation or aggregation affecting the position of the electronic resonance. It is shown that information on the electronic structure of monolayer films is available from the SHG technique when phase measurements are combined with the more conventional SH intensity studies, thus adding a spectroscopic dimension to the technique.

† To whom any correspondence should be addressed.

0953-8984/92/407965+08$04.50

2. Theory

SHG arises from the non-linear polarization $P(2\omega)$ induced by an incident laser field $E(\omega)$. The surface-allowed dipole contribution can be written as

$$P_i(2\omega) = \chi^{(2)}_{ijk} E_j(\omega) E_k(\omega) \tag{1}$$

where $\chi^{(2)}$ is the second-order non-linear susceptibility tensor reflecting the structure and symmetry properties of the surface layer. Large field gradients normal to the surface can also give rise to higher-order bulk non-linear polarization but, under the experimental conditions used, no SHG from the fused silica substrate was detected. The various phenomenological models of surface and interface SHG have been reviewed recently by Heinz [9], and the dependence of the SH intensity from hemicyanine films on the incident angle has been shown to agree well with these models [10]. A three-phase model is used here in determining the SH response of the monolayer and follows the approach of Zhang *et al* [11], which was based on the formalism of Bloembergen and Pershan [12]. The transmission geometry used in this paper requires some changes to the Fresnel coefficients. For a linearly polarized incident wave at frequency ω and with the field vector making an angle α to the plane of incidence, the p and s components of the electric field of the transmitted SH wave are

$$E^{p}_{2\omega}(\alpha) = (A\cos^2\alpha + B\sin^2\alpha + C\sin 2\alpha)E(\omega)^2 \tag{2}$$

$$E^{s}_{2\omega}(\alpha) = (F\cos^2\alpha + G\sin^2\alpha + H\sin 2\alpha)E(\omega)^2. \tag{3}$$

A to H depend on χ_{ijk}, the angle of incidence, θ (45° in this work), the dielectric function of the substrate, ϵ_g, and the dielectric functions of the monolayer, ϵ_1 and ϵ_2, at frequencies ω and 2ω, respectively. Note that the monolayer is assumed to be optically isotropic (the dielectric function comprises a single, frequency-dependent component). The SH intensity depends on the square of the field, $I(2\omega) \propto |E(2\omega)|^2$ and measurements are made of intensity as a function of polarization angle, α. If the monolayer has azimuthal isotropy then (2) and (3) are symmetric about $\alpha = 90°$, and $C = F = G = 0$. Figures 4 and 5 (see later) have this symmetry showing that the monolayers are indeed isotropic. If all parameters are real, then the ratios A/B and H/B are given by

$$\begin{aligned} A/B = \{&[\cos\theta + (\epsilon_g - \sin^2\theta)^{1/2}]^2/[\epsilon_g\cos\theta + (\epsilon_g - \sin^2\theta)^{1/2}]^2\} \\ &\times [(\epsilon_g - \sin^2\theta) + 2(\epsilon_2/\epsilon_1)\epsilon_g\cos\theta(\epsilon_g - \sin^2\theta)^{1/2} \\ &+ \sin^2\theta(\epsilon_g^2/\epsilon_1^2)\chi_{zzz}/\chi_{zyy}] \end{aligned} \tag{4}$$

$$H/B = \epsilon_g^{1/2}(\epsilon_2/\epsilon_1)\chi_{yyz}/\chi_{zyy}. \tag{5}$$

In order to relate the susceptibility, χ, to the molecular hyperpolarizability, β, it is assumed that a single component along the long molecular axis ζ, $\beta_{\zeta\zeta\zeta}$, dominates the non-linear response. Evidence in support of this assumption is discussed in section 4. For an azimuthally isotropic monolayer,

$$\chi_{zzz} = N_s\langle\cos^3\psi\rangle\beta_{\zeta\zeta\zeta} \tag{6}$$

$$\chi_{zyy} = \tfrac{1}{2}N_s\langle\sin^2\psi\cos\psi\rangle\beta_{\zeta\zeta\zeta} \tag{7}$$

where N_s is the surface number density of molecules and ψ is the polar (or tilt) angle of the molecule measured between the substrate surface normal, z, and the long molecular axis, ζ. The angle brackets represent an averaging over the orientational distribution, which is assumed to be narrow for good quality Langmuir–Blodgett monolayers. The average tilt angle of the molecule, $\overline{\psi}$, can be determined from

$$\tan^2 \overline{\psi} = 2\chi_{zyy}/\chi_{zzz} \tag{8}$$

and (4).

Finally, the molecular hyperpolarizability is often estimated by using a simple two-level model, which gives:

$$\beta_{\zeta\zeta\zeta}(-2\omega;\omega,\omega) \propto \{\omega_0/[(\omega_0^2-\omega^2)(\omega_0^2-4\omega^2)]\}\, f\Delta\mu \tag{9}$$

where f is the oscillator strength for the transition, $\Delta\mu$ is the difference in dipole moment between the excited state and the ground state, and ω_0 is the resonance frequency of the two-level system [13].

3. Experiment

The molecules used were from the important class of substituted cyanobiphenyl and cyanoterphenyl thermotropic liquid crystals, the formulae of which are shown below:

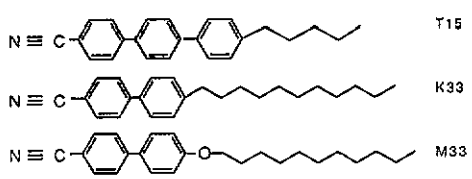

These molecules are structurally unsuited to Langmuir–Blodgett film formation, pure films collapsing at 4.5 mN m^{-1} with K33, and 14 mN m^{-1} with T15. With chloroform as the solvent, M33 forms a cloudy, rigid film on the water subphase. However, good quality monolayers containing 0.36 mole fraction of the liquid crystals in stearic acid can be prepared at room temperature on the triply distilled water subphase. Such films were transferred to a fused silica substrate at a dipping pressure of 30 mN m^{-1}, and with a transfer ratio above 0.95. Only one side of the substrate was coated in these experiments. Linear optical absorption spectra could not be obtained from the monolayers, but fluorescence excitation spectra could be measured on a Perkin–Elmer MPF-44B spectrophotometer.

A frequency-doubled Q-switched Nd/YAG laser was used for the SHG experiments at 532 nm excitation. The pulse length was 15 ns at 20 Hz repetition rate. This was also used to pump a dye laser for excitation at 634 nm. Laser pulse energy was maintained below 10 kJ m^{-2} to avoid any laser-induced desorption or damage effects. At these power densities no SHG was observed from either the substrate or pure stearic acid monolayers, and the SH intensity from the liquid crystal monolayers was typically a few photons per pulse.

The phase change of the SH signal was measured by inserting an x-cut quartz plate in the input beam and rotating it about its y-axis fractionally away from the

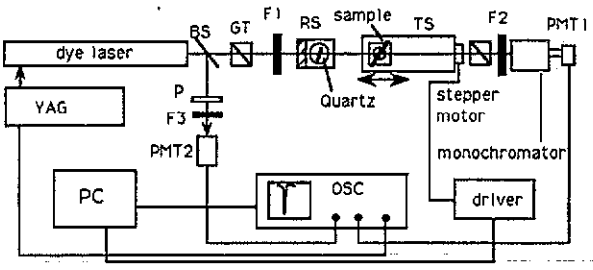

Figure 1. Apparatus for SH phase measurements from the liquid crystal/stearic acid monolayers. Key: RS, two-axis rotation stage; TS, stepper-drive translation stage; OSC, oscilloscope; P, urea powder; GT, Glan–Thompson prism polarizer; BS, beam-splitter; F, filters; PMT, photomultiplier tube; PC, microcomputer.

first minimum of the Maker fringe produced by SHG in the bulk of the quartz [14]. An interference plot can then be obtained by traversing the sample along the beam, while monitoring the combined SH intensity from the sample and the quartz (figure 1). The dispersion in air of the fundamental (refractive index n_ω) and SH signal ($n_{2\omega}$) produces a variation in the optical path length of the two SH signals, allowing their phase difference to be measured [15]. As the phase of the SH signal from the χ_{xxx} component of the quartz reference is known to be zero [16], it is the absolute phase, ϕ, of the SH signal from the molecular monolayer that is measured. This phase is determined by fitting the intensity variation with optical path length, $I_{2\omega}(d)$, to

$$I_{2\omega}(d) = a^2 + b^2 + 2ab\cos[(2\pi d/L_c) + \phi] \tag{10}$$

where a and b are constants, d is the change in path length, and L_c is the coherence length in air, given by

$$L_c = \lambda/[2(n_{2\omega} - n_\omega)] \tag{11}$$

where λ is the excitation wavelength. Figure 2 shows the interference pattern obtained from a K33 sample when the quartz reference is replaced by a second K33 sample such that the two monolayers face each other. Although measurements cannot be made at small displacements due to geometrical constraints, the fit shows that complete cancellation of signal is obtained at the origin, consistent with the π-phase shift expected from the 180° rotation of the molecules between the two sample positions.

Table 1. Parameters for monolayer films containing 36% liquid crystal and 64% stearic acid. Estimated errors are given in parentheses.

Molecule	Fluorescence maximum (nm)	Excitation maximum (nm)	Isotropic?	Tilt angle (deg)	SH phase (317 nm) (deg)	SH phase (266 nm) (deg)	$\lvert\epsilon_2\rvert/\epsilon_1$ (317 nm)
K33	389	295	Yes	28(5)	5(10)	152(10)	1.05(5)
M33	363	305	Yes	27(5)	77(10)	172(10)	1.19(6)
T15	405	325	Yes	0(5)	95(10)	200(10)	—

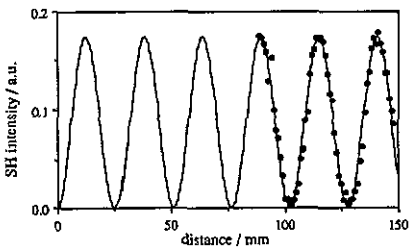

Figure 2. Interference pattern obtained at 317 nm for the K33/stearic acid monolayer, when the quartz reference is replaced by a second K33/stearic acid sample coated on the opposite side. The solid line is a fit to (10). Note the 180° phase shift giving complete destructive interference at the origin.

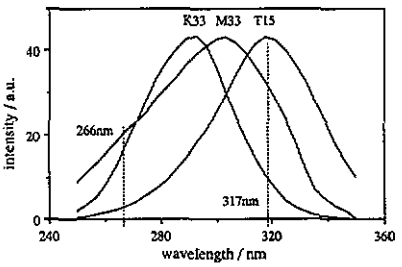

Figure 3. Fluorescence excitation spectrum of the liquid crystal/stearic acid monolayers. The fluorescence was monitored at 389 nm, 363 nm and 405 nm for the K33, M33 and T15 molecules, respectively.

4. Results and discussion

4.1. Linear optical response

The liquid crystal/stearic acid monolayer film parameters are listed in table 1. Figure 3 shows the fluorescence excitation spectra for the three films. The linear optical properties of these films were found to be similar to those obtained from substituted cyanobiphenyls in solution [17]. Increased alkyl chain length, addition of the ether link, or the presence of an extra phenyl group all result in a shift to longer wavelength of the absorption maximum. A small dependence on solvent polarity was also observed, with a shift of less than 10 nm to longer wavelengths as polarity increased. Absorption maxima for homologues of K33 and M33, but two $-CH_2-$ groups lighter, are 281 nm and 297 nm, respectively, in polar solvents, compared with the excitation maxima of 295 nm and 305 nm for K33 and M33 in table 1. The excitation spectra in figure 3 are similar to the absorption spectra in solution, consisting of a broad absorption band without resolved vibrational structure. The fluorescence quantum yield of these liquid crystals is high [17], and it is this which enables the monolayer excitation spectra to be measured.

For the lighter homologues in solution, the electronic transition to the first excited state has been identified as $^1A \rightarrow {}^1L_a$, polarized parallel to the long axis of the molecule [17]. The similar spectra obtained for the higher homologues studied here strongly suggest that the same transition is involved. A large increase in dipole moment has been estimated for this first excited state of the cyanobiphenyls, relative to the ground state [17], and this is one of the necessary conditions for significant SHG, as shown in (9). It follows that the non-linear optical response of these molecules will be dominated, even at resonance, by the single hyperpolarizability component, $\beta_{\zeta\zeta\zeta}$, along the long axis of the molecule.

4.2. Non-linear optical response

Figure 4 shows the variation of p-polarized SH intensity, as a function of input polarization angle, α, for the M33/stearic acid monolayer, while figure 5 is for the s-polarized SH intensity. The solid lines are fits to the square of (2) and (3), respectively. Figures 6 and 7 show typical interference patterns obtained for the

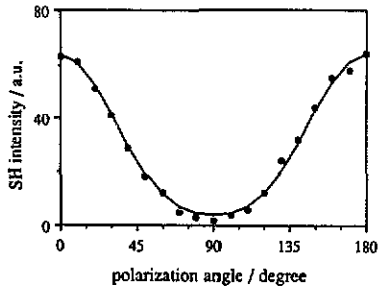

Figure 4. Variation of the p-polarized SH intensity as a function of input linear polarization angle, α, measured from the plane of incidence, for the M33/stearic acid monolayer. The solid line is a fit to the square of (2), and assumes all parameters are real.

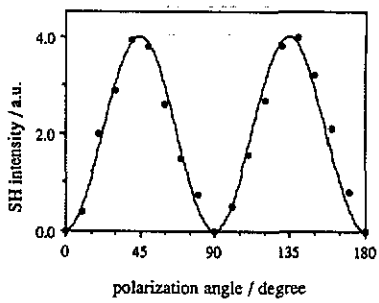

Figure 5. Variation of the s-polarized SH intensity as a function of input linear polarization angle, α, measured from the plane of incidence, for the M33/stearic acid monolayer. The solid line is a fit to the square of (3), and assumes all parameters are real.

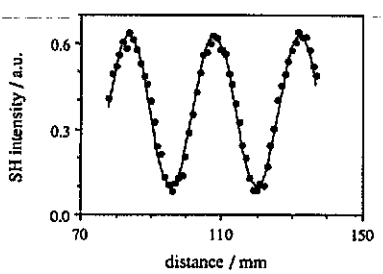

Figure 6. Interference pattern for p-polarized input and output, obtained at 317 nm for the M33/stearic acid monolayer.

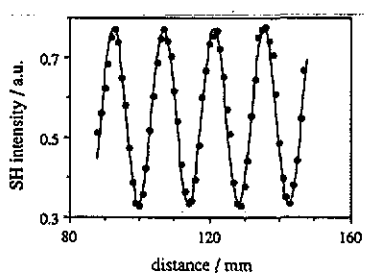

Figure 7. Interference pattern for p-polarized input and output, obtained at 266 nm for the M33/stearic acid monolayer.

M33 system at SH wavelengths of 317 nm and 266 nm, respectively. Similar data were obtained for the K33 and T15 systems. Care must be exercised in extracting structural information using (4)–(8), however, if there are nearby resonances of the system. The linear optical response (figure 3) shows that resonance effects at the SH frequency might be expected for T15 when 634 nm excitation is used, and for K33 with 532 nm excitation. The presence of these excitations near 2ω means that ϵ_2 and χ_{ijk} are likely to be complex (ϵ_1 and ϵ_g remain real), and (4)–(8) require modification. However, the domination of the non-linear optical response of these molecules by a single hyperpolarizability component, $\beta_{\zeta\zeta\zeta}$, along the long axis of the molecule, as discussed above, makes the necessary extension quite simple. In particular, $\chi_{yyz} = \chi_{zyy}$, and

$$|H|/|B| = \epsilon_g^{1/2}|\epsilon_2|/\epsilon_1 \tag{12}$$

with the corresponding expression involving A and B becoming

$$|A|^2/|B|^2 = \{[\cos\theta + \sqrt{a}]^4/[\epsilon_g\cos\theta + \sqrt{a}]^4\}\{[a + b\epsilon_2' + c(\cot^2\overline{\psi})]^2 + (b\epsilon_2'')^2\} \tag{13}$$

where $a = (\epsilon_g - \sin^2\theta)$, $b = 2(\epsilon_g/\epsilon_1)\cos\theta(\epsilon_g - \sin^2\theta)^{1/2}$, $c = 2\sin^2\theta(\epsilon_g^2/\epsilon_1^2)$ and $\epsilon_2 = \epsilon_2' + i\epsilon_2''$. Using the same notation, the phase ϕ (see (10)) of the complex

susceptibility tensor component, χ_{ijk}, is given by

$$\tan\phi = \chi''_{ijk}/\chi'_{ijk} \tag{14}$$

where ϕ is expected to be 90° at resonance, with χ_{ijk} being purely imaginary.

Geometric and electronic structural information can now be extracted. The tilt angle $\overline{\psi}$ of the azimuthally isotropic monolayer can be determined from (13), using 634 nm excitation. $|A|^2$ and $|B|^2$ can be obtained from the α–p data, such as those of figure 4, with $\alpha = 0°$ and 90°, respectively (see (2)). The linear optical constants in (13) are ϵ_g (2.1219 for the fused silica substrates used), together with ϵ_1, ϵ'_2 and ϵ''_2 for the monolayer. While state-of-the-art spectroscopic ellipsometry should have sufficient sensitivity to determine these linear optical constants directly [3], in the absence of such measurements it is still possible to determine $\overline{\psi}$ for these molecules with reasonable accuracy. By expanding (13) it can be seen that the parameters required are ϵ_1, (ϵ'_2/ϵ_1) and $|\epsilon_2|/\epsilon_1$. The last of these can be obtained directly from (12), with $|H|^2$ from the α–s data (figure 5). Table 1 shows the values obtained for $|\epsilon_2|/\epsilon_1$ from K33 and M33, for 634 nm excitation, and it can be seen that the ratio moves away from unity as a resonance is approached. No value could be obtained for T15 because the α–s signal was below detection limits, showing that the tilt angle is near 0°.

The value of ϵ_1 for the films, at frequency ω far from resonance, will be between 1.96 (stearic acid) and 2.30 (T15 monolayer on a silver film, determined by attenuated total reflection at 632.8 nm [18]). The ratio (ϵ'_2/ϵ_1) could vary substantially from unity at resonance, but figure 3 shows that this will be most critical for T15, where this ratio is not required. Tilt angles were calculated for K33 and M33 with ϵ_1 varying between 1.96 and 2.30, and with (ϵ'_2/ϵ_1) varying between 1.0 and 1.5 for K33, and 1.0 and 2.0 for M33, these estimates being based on the $|\epsilon_2|/\epsilon_1$ measurements. The calculations show that these ranges produce only a small spread in angle, because the tilt angle itself is small for these molecules. It is important to note that these linear optical parameters play an increasingly important role as the tilt angle of the molecule becomes larger, for the type of measurement made in this work. Results are presented in table 1, where it can be seen that the K33 and M33 have the same tilt angle of about 27°, within experimental error, while T15 has a tilt angle around zero. The K33 and M33 molecules are very similar in size but T15 has a much shorter alkyl chain and it is suggested that this, together with the flexibility of the terphenyl linkage, allows better packing with the stearic acid molecules, leading to the tilt angle around 0° under these dipping conditions.

Important information on the electronic structure of the molecules comes from the phase of the SH signal. Interference measurements for p-polarized input and output (α–p, with $\alpha = 0°$), such as those of figures 6 and 7, lead to the phase angles reported in table 1. A simple interpretation of the phase is possible here because it has been shown above that $\beta_{\zeta\zeta\zeta}$ dominates the SH response, and so the principal factor determining the phase is $\beta''_{\zeta\zeta\zeta}/\beta'_{\zeta\zeta\zeta}$. The 0°–p experimental configuration produces a SH intensity dependent on $|A|^2$ (see (2)), which involves χ_{zyy} and χ_{zzz} components. Interference measurements for K33 were also compared for 0°–p and 45°–s. This latter SH signal depends on $|H|^2$ ((3) with $F = G = 0$), which involves χ_{yyz}. The difference in phase between these measurements involving three different χ-components was $6° \pm 10°$, which provides strong support for the simple model of domination of the SH response by the $\zeta\zeta\zeta$-component of β.

The phase angles, ϕ, of table 1 can now be easily interpreted by reference to

figure 3. For the SH signal at 317 nm, K33 is away from the resonance which lies at a shorter wavelength, and so $\phi \sim 0°$. M33 is close to the electronic resonance and has $\phi \sim 75°$, while T15 is on resonance with $\phi \simeq 90°$, showing that $\beta_{\zeta\zeta\zeta}$ for T15 is purely imaginary. In contrast, the SH signal for the molecules at 266 nm has moved through the resonances, which now lie at longer wavelengths. T15 and M33 are now further from resonance and ϕ is near 180° for these, while K33 is now closer to the resonance with $\phi \simeq 150°$. The phase is expected to differ by 180° across a resonance, like a driven simple harmonic oscillator, and this produces a sign change in $\beta_{\zeta\zeta\zeta}$ (see (9)).

Finally, quantitative estimates of $\beta_{\zeta\zeta\zeta}$ are not given here because local field effects need to be properly evaluated [9]. A study of the dependence of the SH response on the liquid crystal concentration in the stearic acid LB film is currently under way [19].

5. Conclusions

Comparison of the linear and non-linear optical response of molecular monolayers has shown that substantial geometric and electronic structural information can be extracted from the SH response. The combination of SH intensity and phase measurements provides much more information than intensity studies on their own, and adds an important spectroscopic dimension to SHG from molecular monolayers.

Acknowledgments

Z-R Tang is a University of Dublin Adam Loftus Scholar. Experimental assistance from J D O'Mahony, M Cavanagh and E F Walsh is acknowledged.

References

[1] Shen Y R 1989 *Nature* **337** 519
[2] Richmond G L, Robinson J M and Shannon V L 1988 *Prog. Surf. Sci.* **28** 1
[3] McGilp J F 1989 *J. Phys.: Condens. Matter* **1** SB85; 1990 *J. Phys.: Condens. Matter* **2** 7985
[4] Chang R K, Ducuing J and Bloembergen N 1965 *Phys. Rev. Lett.* **15** 6
[5] Tom H W K, Heinz T F and Shen Y R 1983 *Phys. Rev. Lett.* **51** 1983
[6] Kemnitz K, Bhattacharyya K, Hicks J M, Pinto G R, Eisenthal K B and Heinz T F 1986 *Chem. Phys. Lett.* **131** 285
[7] Kelly P V, O'Mahony J D, McGilp J F and Rasing Th 1992 *Appl. Surf. Sci.* **56–8** 453; 1992 *Surf. Sci.* **269/270** 849
[8] Berkovic G, Shen Y R, Marowsky G and Steinhoff R 1989 *J. Opt. Soc. Am.* B **6** 205
[9] Heinz T F 1991 *Nonlinear Surface Electromagnetic Phenomena* ed H-E Ponath and G I Stegeman (Amsterdam: North-Holland) ch 5
[10] Hollering R W J and Teesselink W J O V 1990 *Opt. Commun.* **79** 224
[11] Zhang T G, Zhang C H and Wong G K 1990 *J. Opt. Soc. Am.* B **7** 902
[12] Bloembergen N and Pershan P S 1962 *Phys. Rev.* **138** 606
[13] Zyss J and Chemla D S 1987 *Nonlinear Optical Properties of Organic Molecules and Crystals* ed D S Chemla and J Zyss (Orlando, FL: Academic) ch II-1
[14] Maker P D, Terhune R W, Nisenoff M and Savage C M 1962 *Phys. Rev. Lett.* **8** 21
[15] Shen Y R 1984 *The Principles of Nonlinear Optics* (New York: Wiley) p 99
[16] Weber M J 1986 *Handbook of Laser Science and Technology* vol III, part 1 (Boca Raton, FL: Chemical Rubber Company) p 44
[17] David C and Baeyens-Volant D 1980 *Mol. Cryst. Liq. Cryst.* **59** 181
[18] Tang Z-R and McGilp J F 1991 unpublished work
[19] Tang Z-R and McGilp J F 1992 to be published